

TABLE 2. Count rates ($e^- s^{-1} \text{Å}^{-1}$) for monochromatic magnitude $m_\lambda = 12.0$.

λ (nm)	Grism #6	Grism #7
350	41	–
400	69	52
450	56	59
500	48	61
550	–	58
600	–	52
650	–	48

data are transferred seamlessly and with all necessary header information right into the observer's favorite image-processing system.

Another important goal is to add a direct CCD imaging option. Finer sampling is needed to yield the best spatial resolution on nights of good seeing (which

will, we hope, be more frequent with the new mirror cooling system). Also, focal reducing optics are not always optimal for precision field photometry. Therefore, we plan to install, perhaps in early 1996, a direct CCD of the type described above in a stand-by position in the adapter, fed by a 45° mirror and with rapid tip/tilt correction for atmospheric image motion. At $0.''23$ per pixel, this should be a valuable high-resolution imaging option, always readily available when good seeing occurs.

Moreover, a fiber-feed position is foreseen in the adapter, so an off-telescope instrument can be permanently connected, eliminating changeovers and improving instrument stability. Options under study include the radial-velocity scanner CORAVEL or (better) an optimized, bench-mounted échelle spectrograph.

Finally, much remains to be learned about the optimization (including UV flooding), testing, maintenance, and operation of high-performance CCD detectors. We look forward to continuing our pleasant cooperation with the ESO Optical Detector Group in this area, to the benefit of both sides – and our users.

Acknowledgement

The DFOSC, CCD development, and telescope upgrade projects were made possible by generous financial support from the Carlsberg Foundation and the Danish Natural Science Research Council.

For further information please contact: J. Andersen, Copenhagen University, Denmark, e-mail: ja@bro835.astro.ku.dk

A New CCD Field Lens in EMMI Red Arm

R. GILMOZZI, B. DELABRE, S. D'ODORICO, J.-L. LIZON, O. IWERT, P. GITTON, S. DEIRIES, ESO-Garching

The ESO Multi-Mode Instrument EMMI was first installed at the NTT in the summer of 1990. At that time the red arm was equipped with a thick CCD with UV-blue sensitive coating because the originally planned thinned 2048^2 detector had not become available. At the beginning of 1994 (see *The Messenger* No. 76, p.15) a 2048^2 thinned SITe CCD was finally installed on the instrument with its dedicated camera. One last step was however still necessary to fully realize the planned optical quality of the instrument. The sensitive surface of the CCD delivered to ESO proved to be convex with a peak at its centre in the direction of the camera. The curvature is due to the CCD assembly process and it is well approximated by a paraboloid. The difference between centre and corners is approximately $200 \mu\text{m}$ and resulted in a higher dispersion around the average value of the image quality in the field of view, with a significant degradation in the corners. A new field lens, to serve also as window of the cryostat, was computed to compensate for this curvature and it has been installed and tested in three nights in January 1995.

Image quality has been determined through observations of several star fields (either outer regions of globular clusters, or open clusters) in order to determine the best centring position for the field lens. One important point to realize is that image quality can be really assessed only through astronomical observations per-

formed in good seeing. NGC 2204 appeared to be the best choice in terms of uniform star distribution. After several iterations of fine-centring the lens, an image of $0.57''$ was obtained (i.e. just above

the critical sampling for the $0.27''$ pixels of the camera). Although a 10 % variation was visible between centre and edges of the field of view, this demonstrated that the performance of the lens allows us to

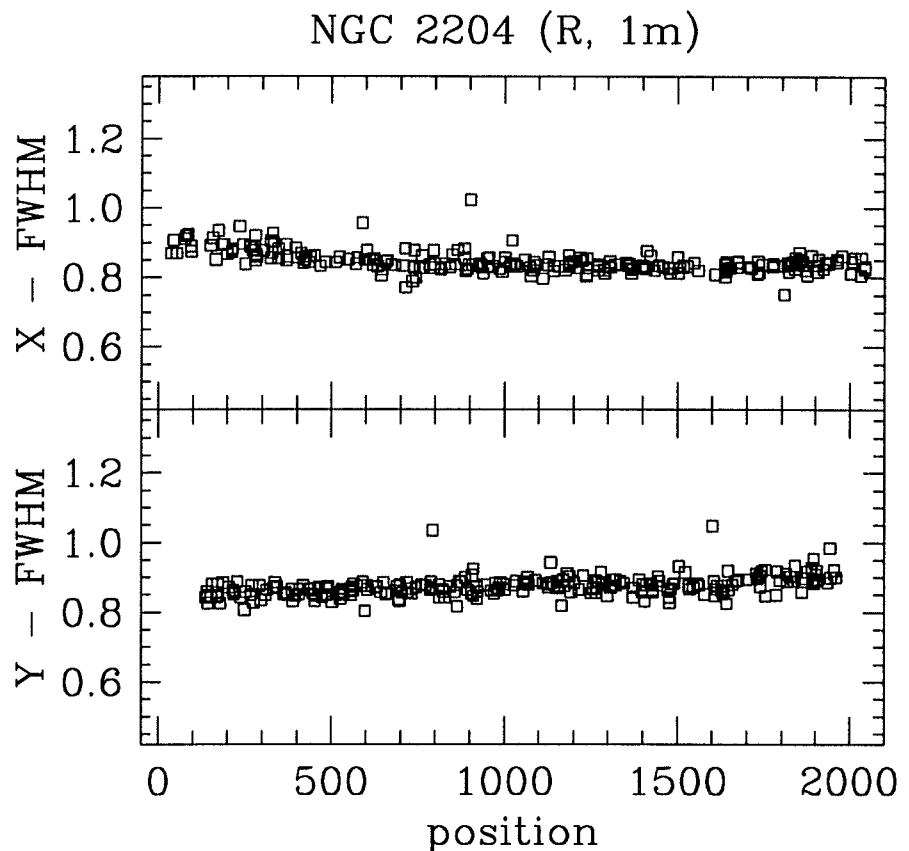


Figure 1: Distribution of the stellar FWHM as a Function of position.



Figure 2: 40-min $H\alpha$ image of the recurrent nova *T Pyx* in $0.7''$ seeing. The image is $80'' \times 80''$.

reach an image quality close to the best seeing values ever measured at the NTT. Figure 1 shows the variation of the Point Spread Function as a function of position for the best (and final) lens position (NGC 2204, R filter, 1 minute integration). The average value of the FWHM is 0.84 (0.87) ± 0.02 arcseconds in x (y) – of course, the $0.57''$ seeing would not last!

A very small effect at the edges of the chip is still present (of the order of 5%), but it is not clear whether it is due to the new field lens: during the tests it became apparent that both the position of the rotator and the zenith distance can affect the image quality (for a discussion of the latter effect, which is also the cause of the slight ellipticity of the star images and which will be further analysed – and possibly corrected – in February, see “NTT Bits and Pixels” in this issue). In the worst case, these effects can amount to at most 10–15% at the edge of the field of view, a value still quite acceptable, especially in view of the very large field of view of this camera ($9' \times 9'$). A more thorough analysis of the dependence on rotator position of the instrument flexure and of the camera triplet (see “NTT Bits and Pixels”) will be performed in the near future in order to quantify and understand these effects and to try to reduce even further the spread of the FWHM as a function of position.



Figure 3: Full field of view ($9' \times 9'$) image of NGC 1850, a young double cluster in the LMC, in the light of [NII]. The filamentary structures are most likely supernova remnants.

A preliminary value of the plate scale was obtained by comparison of a $2' \times 2'$ image portion with an HST WFPC2 image for which astrometry was available. Though a determination of the plate scale based on the full field of view will be produced, the derived value of 0.2698 ± 0.0002 arcsec per pixel shows that the new lens has not introduced any substantial changes. However, users should be aware that images taken prior to the lens change cannot be used as they are for preparing MOS plates: a scale change of 8% is present between images taken before and after the replacement. Old and new images can be successfully coadded if the old ones are rebinned by 0.99187.

The efficiency of the camera has also not changed with respect to the value prior to the installation of the new lens (to within the uncertainties): the numbers of $e^- s^{-1}$ for a 15^m A star are 20,600 (V), 24,000 (R), 12,700 (I), to be compared with the previous 18,900 (V), 22,000 (R), 11,900 (I) (J. Storm 1994).

Focusing of the telescope should be preferentially done in the inner 1000×1000 pixels of the frame, since the focus wedge gives, at the edges, a large dispersion of values.

We also tested the stability of the image quality over longer integrations, with results very similar to those of Figure 1.

Figure 2 shows a 40-minute H α image of the recurrent nova T Pyx. The FWHM of stellar images is 0.7", one of the best ever attained for such a long exposure time through a narrow-band filter. The image shows in exquisite detail the debris from a previous outburst and will be used together with spectral information to determine to which historical outburst the sur-

rounding material refers, and hence to derive a new, better estimate of the distance. Figure 3 is a 0.9" seeing, 30-minute [NII] image of the young double cluster NGC 1850 in the LMC and shows extended filamentary emissions around the cluster. These are very likely the remnants of supernova explosions in the main cluster, which is only 50 million

years old. Shock waves from supernova explosions were invoked as the probable cause of the formation of the much younger companion cluster (*Ap. J. Lett* 435 L43).

For further information please contact:
R. Gilmozzi, ESO-Garching,
e-mail: rgilmozz@eso.org

Ghost Analysis and a Calibration Database for the Long Camera of the CES

L. PASQUINI, H.J. ARAYA, ESO-La Silla

1. Introduction

We present recent improvements and changes at the CAT and CES, mostly performed during the telescope idle period in September 1994. We also describe a new calibration database which has been installed in La Silla computers and an analysis of the ghosts found in our extensive tests.

2. CAT Telescope

The floor of the CAT dome was in a bad shape and unsafe for observers and night assistants. The floor panels were replaced.

The CAT telescope and the CES spectrograph were re-aligned and the primary mirror of the telescope adjusted. This intervention was requested to improve the CAT optical quality, in particular to minimise coma; with this intervention also a more stable and accurate pointing model has been achieved.

3. CES Spectrograph

Due to a major technical problem (abnormally high read-out noise) on CCD #30, mounted on the CES Long Camera, this was replaced by CCD #34 in October 1994.

The CES spectrograph was used, in combination with the Long Camera and CCD #30, to acquire a full set of calibration spectra. 140 Th-Ar and Flat Field calibrations were recorded with the RED path covering the range between 8990 and 5215 Å, while 80 frames were acquired with the BLUE path covering the 5200–3790 Å domain. In Table 1 and 2 a summary of the wavelength interval steps used in the RED and BLUE path is given.

The aim for the acquisition of the calibration data set was twofold:

(1) To allow an analysis of the spectrograph ghosts present in the wavelength domain commonly used by the observers.

TABLE 1: Summary of central wavelengths and steps used for the calibrations in the RED domain.

λ_c Beg	λ_c End	Step (Å)
8890	8500	70
8435	8110	65
8050	7330	60
7275	6670	55
6620	6070	50
6025	5925	50
5880	5340	45
5295	5215	40

TABLE 2: Central wavelengths and steps used for the calibrations in the BLUE domain.

λ_c Beg	λ_c End	Step (Å)
5200	4520	40
4485	4030	35
4000	3790	30

(2) To provide the potential CES users with a complete set of calibration data, to be used to better planning their observations.

We note that, although the presence of ghosts is known to be more serious when using the CES in combination with the Short Camera, we have preferred to perform the calibration set with the Long Camera, mainly because, as soon as a new thinned detector will be available at La Silla (March 1995), the Short Camera will be decommissioned and only the Long Camera will be offered to the users.

The spectra were acquired with a nominal resolving power $R=10^5$ and a decker height of 5 arcsec. Although the CES users are recommended to use a longer

decker, a short decker was preferred because this facilitates the separation of those Flat Field (FF) ghosts falling close to the science spectrum.

The central wavelengths of the calibration frames were chosen to ensure some overlap between adjacent spectral ranges. The FF exposures integration times were selected to give a peak intensity level around 10,000 ADU (one ADU corresponds to 2.8 electrons in the used configuration) in the extracted spectra, and the intensity maximum typically varies between 6000 and 14,000 ADU after extraction. Only at very blue wavelengths (i.e. below ~ 4000 Å) lower exposure levels were obtained, because the maximum duration of the FF exposures was fixed to two minutes.

Th-Ar integration times were set to obtain a level of at least 10,000 ADU in the strongest lines of the extracted frame.

One-dimensional spectra were extracted over a slit of 13–14 pixels, almost the whole slit height.

Because these frames may be very useful for the CES users to prepare their observing runs and calibrations, they are made available to the users' community. Both the original (2-dimensional) and the extracted (1-dimensional) files are stored as FITS files; they can be accessed and copied through ftp with the following commands:

```
ftp 134.171.81.6
username: anonymous
password: your ident as password
cd pub/ces/calib
get README
binary
get M $\lambda_c$ .ND
```



Figure 1: Two-dimensional image of the Th-Ar exposure centred at 6470 Å.